STATUS OF ITALIAN TEST DATA ON SEISMIC ISOLATORS AND COMPARISON WITH COMPUTER PREDICTIONS

M. Forni and A. Martelli, ENEA, Bologna, Italy
A. Dusi and F. Bettinali, ENEL S.p.A. - CRIS, Milano, Italy

ABSTRACT

In this paper the reliability of finite element model (FEM) for simulating the behaviour of high damping rubber bearings (HDRBs) is presented. R&D work on seismic isolation development and application, with particular regard to the numerical modelling, is in progress in Italy and encouraging results have already been obtained. Recentely, 'optimized' and 'further optimized' isolators were designed, manufactured and tested in the framework of a co-operation among Italian and European partners (ENEL et al., 1993). For all the devices, numerical investigations have been carried out up to very large strains and the response of the FEMs has been verified against experimental evidence.

1. INTRODUCTION

The HDRBs are formed by alternated vulcanized rubber layers and steel plates, bonded together by use of chemical compounds. They are usually placed between the structure and its foundations. Their features provide high stiffness in the vertical direction, to support the dead load of the superstructure, and low stiffness in the horizontal plane, thus minimizing amplification of ground acceleration, leading, however, to large horizontal displacements during strong earthquakes (Forni et al., 1996).

In literature many contributions concerning rubber-like finite element modelling are available. These are generally concerned with the theoretical problem of dealing with an incompressible material, whereas the proposed finite element analyses of elastomeric bearings are very few.

The mechanical behaviour of these devices is difficult to be modelled because of the high geometrical and mechanical nonlinearities and the incompressible behaviour of the rubber which characterize the problem.

For each type of modelled isolator (§ 2), analyses have been performed up to very large (even 450%) shear strains, in order to evaluate the behaviour of the bearings in a range close to their failure or instability. Results from finite element analyses have been compared with the experimental ones obtained in the framework of an experimental investigation which has been widely reported by Martelli et al., 1996.

2. BEARINGS CONSIDERED

Analyses were carried out by considering two kinds of rubber compounds (soft and hard), two different primary shape factors S (that is the ratio between the loaded and the unloaded areas of a single rubber layer) and five different kinds of attachment systems (Forni et al., 1995). However, due to space limitation, only the numerical analyses carried out by considering the recess and the bolts & central dowel attachment systems are reported herein.

2.1 Optimized HDRBs

In the framework of research activities involving ENEL, ENEA and other partners (ENEL et al., 1993) a considerable number of optimized HDRBs were designed, manufactured and tested in Italy. These isolators are characterized by:

a) two different rubber compounds: harder (shear modulus G=0.8 MPa) and softer (G=0.4 MPa);
b) two values of the primary shape factor (S = 12 and S = 24);
c) three different geometric scales (diameter D = 125, 250 and 500 mm);
d) two different attachment systems (recess and bolts & dowel).

The devices were produced by ALGA and experimentally tested at ISMES laboratory.

The optimized bearings analized using the finite element technique and reported herein, had an overall diameter of 250 mm and both shape factors of 24 and 12. In the case of the higher shape factor, there were 30 layers of elastomer (G = 0.8 MPa), each being of 2.5 mm thick, alternated with 29 steel shims of 2 mm thickness. The steel end plates were 15 mm thick and had a 240 mm diameter. The total height was 114.5 mm. The bearing having S = 12 was formed by 15 layers of rubber (G = 0.8 MPa), each being of 5 mm thick, sandwiching 14 steel shims of 2 mm thickness. The steel end plates were again 15 mm thick, with a diameter of 240 mm. Both the bolts & dowel and the recess attachment systems were considered.

2.2 Further optimized HDRBs

Tests and FE calculations performed on the so-called optimized HDRBs (ENEL et al., 1993) showed the possibility of further improving their stability at large deformations by decreasing their height. Therefore, some 'further optimized' HDRBs were designed by ENEA and produced by ALGA. Several kinds of these devices were manifactured by combining two different shape factors (S = 12 and S = 24), two rubber compounds (G=0.8 and 0.4 MPa), two attachment systems (recess and bolts & dowel) and two geometric scales (D=250 and 125 mm).

The 'further optimized' bearing analyzed in this study had an overall diameter of 125 mm and a shape factor of 12. There were 12 layers of elastomer (G = 0.4 MPa), each 2.5 mm thick, alternated with 11 steel shims of 1 mm thickness. The steel end plates were 10 mm thick and had a 120 mm diameter. The total height was 61 mm. These devices were used to seismically isolate a four-storey steel frame which, considering different geometrical configurations, has been tested on the shaking table (Forni et al., 1996).

Figure 1 reports a sketch of a 'further optimized' HDRB with a diameter of 250 mm and a total rubber height H of 60 mm. In figure 2, an isolator during a compression test performed using SISTEM (Seismic ISolator TEst Machine) is reported (Martelli et al., 1996).

3. FINITE ELEMENT MODELLING

The behaviour of the bearings under vertical load and shear strain has been modelled by means of finite element analyses, performed using the ABAQUS code, version 5.5 (ABAQUS, 1995).

3.1 Material models

The mechanical behaviour of rubber-like materials is described in ABAQUS by means of an elastic, isotropic and approximately incompressible model. The governing constitutive equations are derived assuming the following polynomial form (Rebelo, 1991) for the strain energy function U:

$$U = \sum_{i+j=1}^{N} C_{ij}(\bar{I}_1 - 3)^i(\bar{I}_2 - 3)^j + \sum_{i=1}^{N} \frac{1}{D_i}(J_{el} - 1)^{2i} \qquad (1)$$

being $\bar{I}_1$ and $\bar{I}_2$ the first and the second invariants of the deviatoric strain, J the elastic volume ratio, C_{ij} and D_i material constants and N the order of the energy function. The value of the constants D_i determines the compressibility of the material and is set equal to zero for fully incompressible materials. The choice of N (generally N = 1, 2, 3) provides polynomial forms of strain energy more or less complex.

The coefficients in (1) can be defined by the data of experimental tests involving simple state of deformations and stress. Uniaxial, biaxial and shear experiments were used (Ogden, 1984; Rebelo, 1991 and Forni et al., 1995) to determine the above mentioned constants. For all the different compounds analyzed in this study, the characterization tests on rubber specimens have been carried out at ENEL-CRIS laboratories (Bettinali et al., 1996). In the numerical analyses reported in this paper the material was assumed to be incompressible ($D_i = 0$) when studying shear deformations and a polynomial N=2 form was adopted.

As regards the steel shims, an elastic-plastic constitutive behaviour was assumed.

3.2 FE discretization

The difficulties encountered dealing with the incompressibility of rubber-like materials were treated by means of a mixed FE formulation. Hybrid elements have been used; in these elements the pressure stress is independently interpolated from the displacement field, making the numerical formulation of the variational problem well-behaved. An updated Lagrangian formulation is adopted.

Analyses carried out using several kinds of FE models showed (Dusi et al., 1995 and Forni et al., 1995) that rubber layers can be successfully modelled with eight-node elements (C3D8H - ABAQUS Manuals, 1995), which provide linear displacement and constant pressure interpolations, and steel plates with eight-node elements using reduced integration and linear displacement (C3D8R).

At least 8 subdivisions along the radius, 32 subdivisions along the external circumference were employed in the meshing; each rubber layer had three C3D8H elements through its thickness while each steel shim had only one C3D8R element through the thickness.

When modelling the recessed bearings, better results have been obtained using hybrid triangular elements (C3D6H), with six nodes, linear displacement and constant pressure, placed at the inner and outer borders of the bearing.

Pre-processing of the geometry, boundary conditions, materials properties and loads were undertaken using GENESIS (Dusi et al, 1995), a pre-processor for ABAQUS, which is capable of automatically generating the rather complicated ABAQUS input file on the basis of a few input data.

The geometry of the devices and the loading conditions make the problem symmetric. Therefore only one half of the bearing is usually modelled (figure 3-a), by imposing appropriate boundary conditions on displacements and rotations of the nodes belonging to the plane of symmetry. The problem is also hemi-symmetric with respect to the plane parallel to the bases of the device and containing its center of mass. In this paper the authors are therefore proposing the modelling of only a quarter of the device to be analyzed (figure 3-b). Deformations of the HDRBs considered in this work pointed out that a further hemi-symmetry condition can be taken into account in the FE modelling of these devices. An hemi-symmetry about the straight line lying in the hemi-symmetry plane and perpendicular to it exists. Hence, appropriate constraints are invoked along the line of symmetry. In spite of a significant reduction of computational effort required to run the 3D models, the comparison between the results obtained following this approach and those obtained from the modelling of half a bearing, shows that the considered FE models are equivalent from the global response point of view, as shown by figure 3-c.

3.3 FE analyses

Appropriate boundary constraints were applied to the models to simulate the actual service conditions: each bearing was first compressed with the relevant compressive load, then sheared by keeping the vertical force constant until the target value of shear strain was reached.

In order to reproduce the experimental conditions of the bolted device, the FE models assume that the top and bottom faces of the bearings are constrained to remain parallel. While the base plate nodes are fully constrained, every node of the top plate is tied, by means of constraint equations, to a pilot node located at the center of the device; either the vertical and the horizontal loads are then applied to this pilot node.

The recess attachment system is more difficult to be modelled because it involves sliding of a deformable body (the bearing) against a rigid body (the recess plate). In this work, the contact problem was solved by meshing the recess plate' surface using rigid surface elements (IRS4).

4. FINITE ELEMENT ANALYSES: RESULTS AND DISCUSSION

4.1 Optimized HDRBs

The actual experimental test on the 1:2 scale bolted bearing, having a shape factor of 24, subjected to a vertical load of 400 kN (in the case of harder compound) and a horizontal displacement of 225 mm, namely 300% shear strain, is shown in figures 4-a, while in figure 4-b the deformed FE mesh is reported. The 3D numerical model provides deformation and values of stiffness well matching the experimental data (figure 4-c).

Figures 5-a, b, c and 6-a, b, c show the results obtained for 1:2 scale bearings with recess attachment system, respectively for a S=24 device, subjected to a vertical load of 40 t and to 200% shear strain, and for a S=12 bearing under 40 t of vertical load and 300% shear strain.

The deformed configurations provided by the FE models, shown in figures 5-b and 6-b, simulate the actual behaviour of the device well. In both cases the agreement between numerical and experimental horizontal stiffnesses is good.

4.2 Further optimized HDRBs

A comparison between the experimental data and the deformed mesh for the 1:4 scale bolted bearing, subjected to a vertical load of 50 kN and a horizontal displacement of 120 mm, namely 400% shear strain, is reported in figures 7-a and 7-b.

The agreement between numerical and experimental results is quite good. It has however to be observed that, at high shear deformations, the simulated response exhibits a lower shear stiffness with respect to the experimental one. This is probably due to the hyperelastic model implemented for this compound. The coefficients for the polynomial form of the strain energy function (1) were defined from shear tests performed on rather narrow specimens: in these conditions boundary effects could become significant at shear strain higher than 200%, thus leading to a softer behaviour.

5. FUTURE WORK

Accelerated ageing tests on 125 mm diameter optimized bearings are in progress in a climatic chamber, at 70 °C for 4 months, corresponding to an actual ageing of well more than the prescribed 60 years (ENEL et al., 1993). These devices will be subjected to compressive and shear strain experimental tests in order to evaluate the effects of ageing. Rubber specimens, which will be used for the evaluation of the ABAQUS hyperelastic model coefficients, will

also be subjected to the same ageing. Future work will therefore address the implementation of a hyperelastic model of aged rubber and its validation against experimental data.

6. CONCLUSIONS

In this paper the finite element modelling of elastomeric bearings subjected to vertical load and horizontal displacement has been analyzed and verified against experimental evidence.

The extensive numerical simulation aimed at investigating the effects of the numerous variables of the problem has put into evidence which type of material model, discretization and elements have to be adopted in order to obtain a good correlation with the experimental results at very large strains. The distribution of stress in steel shims, the bearing's axial stiffness, the horizontal stiffness are becoming more clearly understood.

The finite element formulation of rubber elasticity, as incorporated into ABAQUS, has been demonstrated, by comparison with experimental results, to be a powerful tool for modelling the behaviour of HDRBs.

Particular attention should be devoted to the experimental tests on rubber specimens (expecially the planar deformation ones) in order to avoid slip or boundary effects which can affect the solution of the problem.

This study demonstrated that ABAQUS can be effectively utilized as an analytical tool for design optimization prior to committing resources to full production and for some qualification purposes.

REFERENCES

ABAQUS Manuals, 1995, Version 5.5, Hibbitt, Karlsson & Sorensen Inc., Providence, Rhode Island, USA.

F. Bettinali, D. Cazzuffi, A. Dusi, L. Fede, 1996, *Valutazione delle caratteristiche di mescole in gomma naturale utilizzate per la costruzione di isolatori sismici,* ENEL S.p.A.-CRIS Internal Report n° 5187 (in Italian).

A. Dusi, M. Forni, 1995, *FE models of steel laminated rubber bearings,* Proc. 6th National Congress of ABAQUS Users' Group Italia, Bologna, Italy.

A. Dusi, R. Cadei, 1996, *GENESIS: a pre-processor for the implementation of 3D FE models of seismic isolators,* ENEL S.p.A.-CRIS internal report n° 5283.

ENEL, ALGA, DYWIDAG, ENEA, MRPRA, SHW, STIN, 1993, *Optimization of design and performance of High Damping Rubber Bearings for seismic and vibration isolation,* EC Contract BRE2-CT93-0524, Project BE7010, Bruxelles, Belgium.

M. Forni, A. Martelli, A. Dusi, G. Castellano, 1995, *Hyperelastic models of Steel-laminated Rubber Bearings for the seismic isolation of civil buildings and industrial plants,* Proc. ABAQUS Users' Conference, Paris, France, 31 May-2 June.

M. Forni, M. Indirli, A. Dusi, A. Brasina, M. Carinci, P. Diotallevi, V. Rebecchi, L. Grassi, 1996, *Seismic analysis of base-isolated structures,* Proc. ABAQUS Users' Conference, Newport, R.I.,USA.

A. Martelli, M. Forni, F. Bettinali, A. Marioni, G. Bonăcina, 1996, *Overview on the progress of Italian activities for the application of seismic isolation,* Proc. of the ASME-PVP Conf., Montreal, Canada, July 21-26

R. W. Ogden, 1984, *Non-linear elastic deformations,* Ellis Horwood Limited, Chichester.

N. Rebelo, 1991, *Analysis of rubber compound with ABAQUS,* Proc. 2nd National Congress of ABAQUS Users' Group Italia, Bologna, Italy.

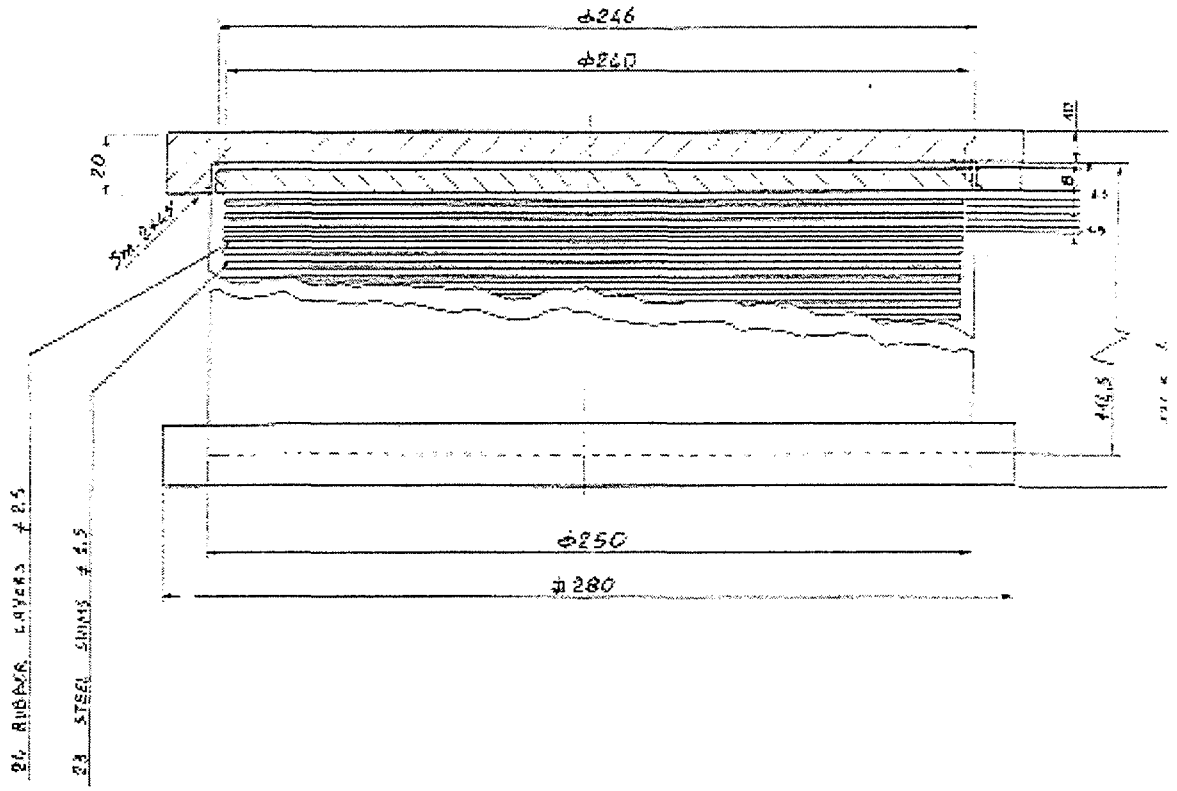

Figure 1. 'Further optimized' HDRB (250 mm diameter, 60 mm total rubber height, recess attachment system)

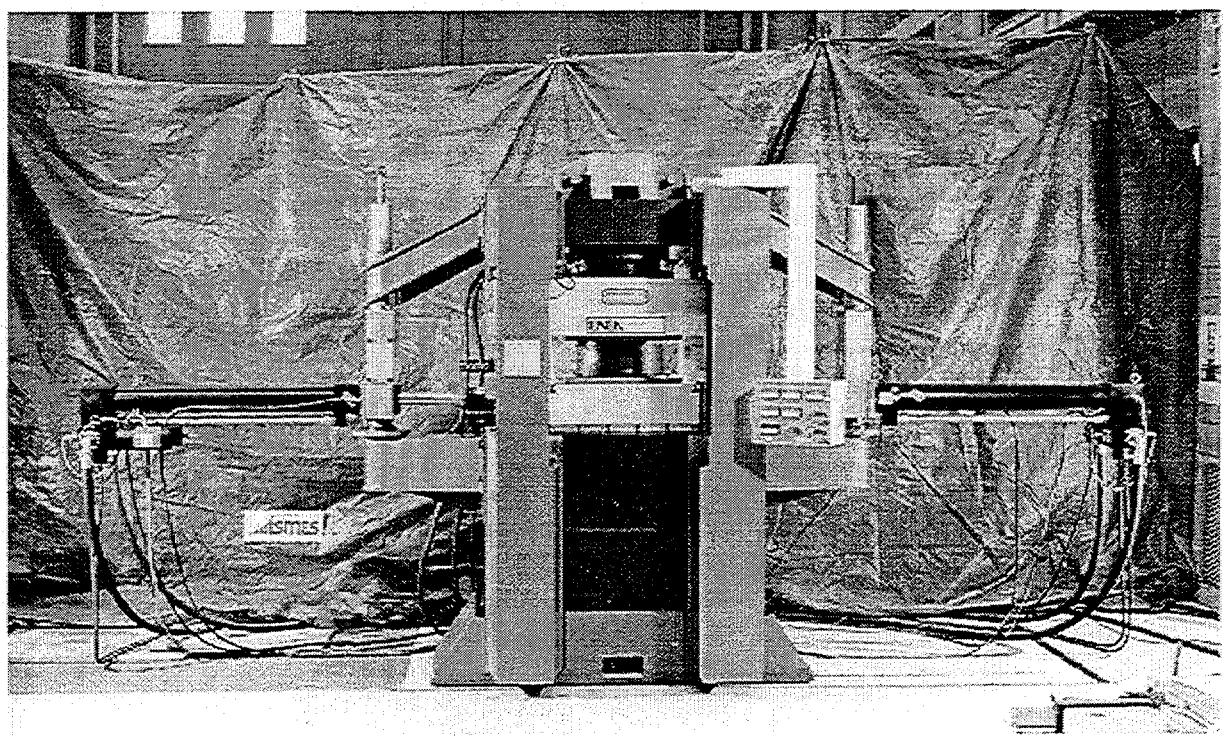

Figure 2. Optimized HDRB under testing on SISTEM machine.

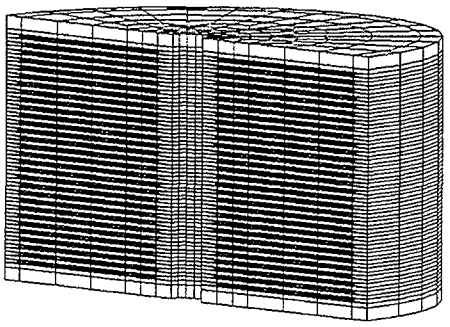

Figure 3-a. FEM of HDRB with symmetry about a vertical axial plane (YSYMM conditions) - Half model

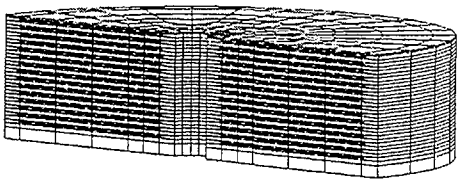

Figure 3-b. FEM of HDRB with symmetry about a vertical axial plane and hemi-simmetry - A quarter model

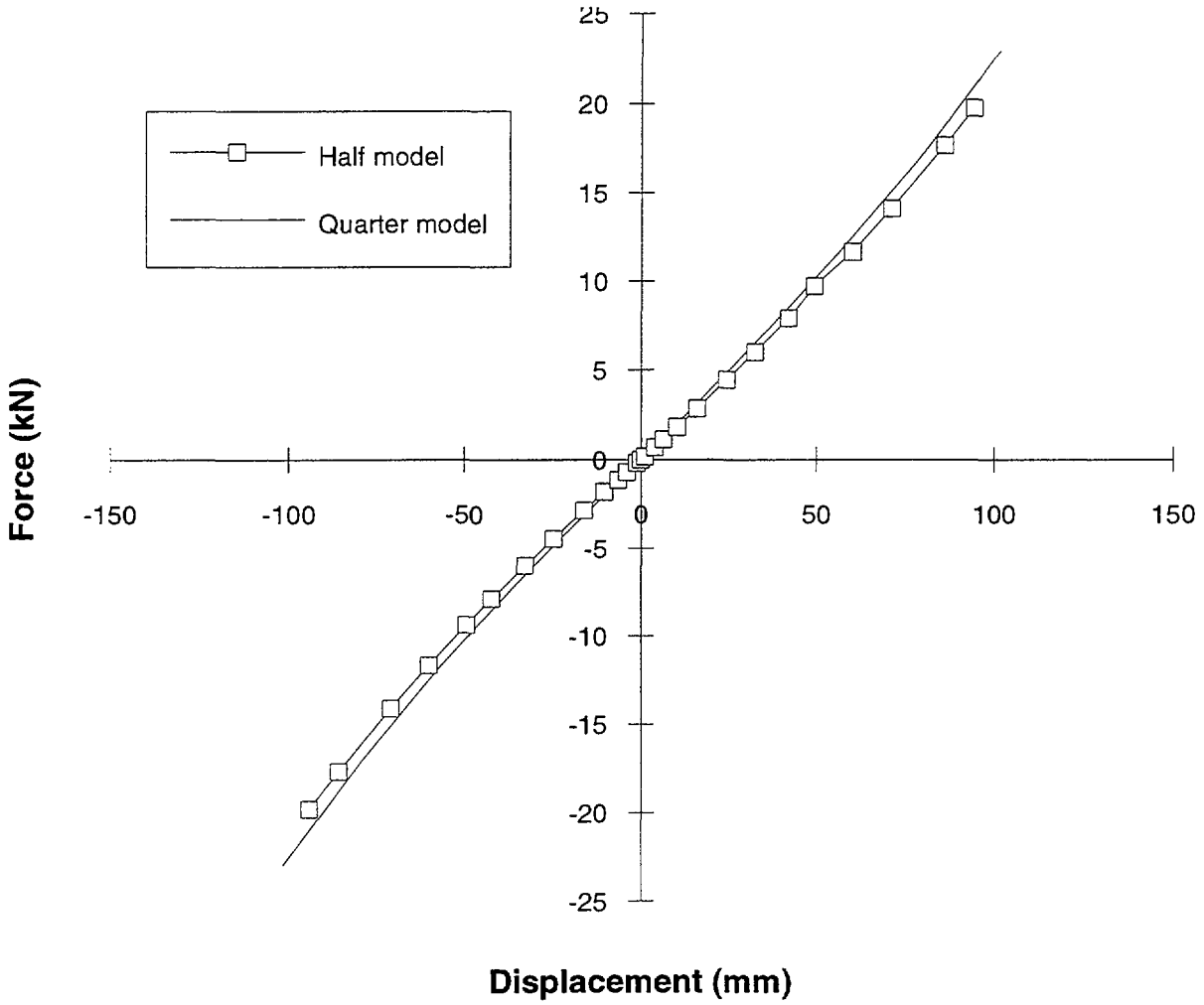

Figure 3-c. Comparison between the horizontal stiffnesses of HDRB in half scale using the FEMs of figures 3-a and 3-b

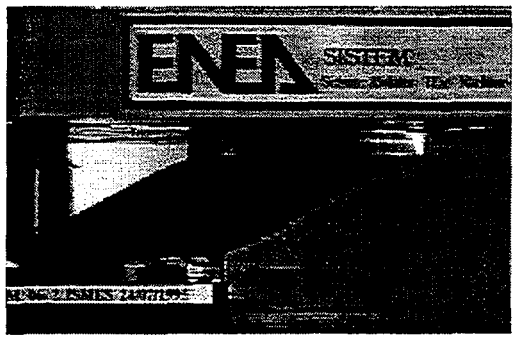

Figure 4-a. Compression and shear test at 300% on a bolted 'optimized' HDRB

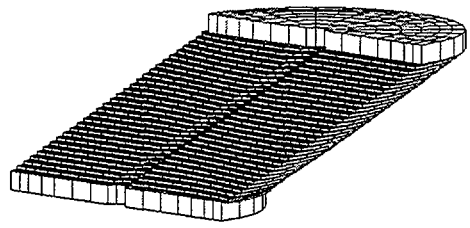

Figure 4-b. FEM of a bolted optimized HDRB at 300 % shear strain

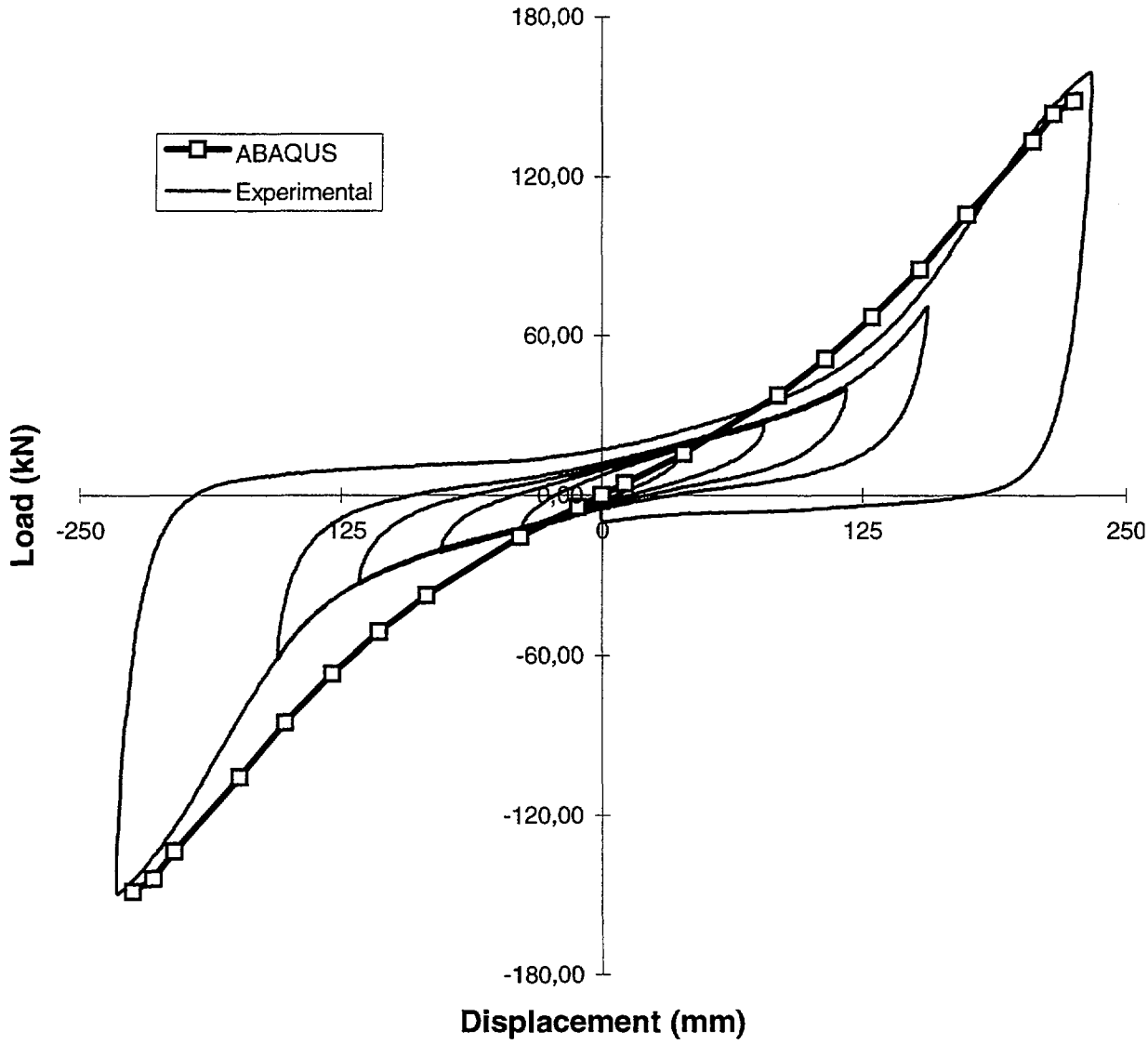

Figure 4-c. Experimental and numerical force-displacement values for a combined compression & 300% shear strain test on a bolted 'optimized' HDRB (1:2 scale, diameter=250 mm, H=75 mm, S=24, G=0.8 MPa)

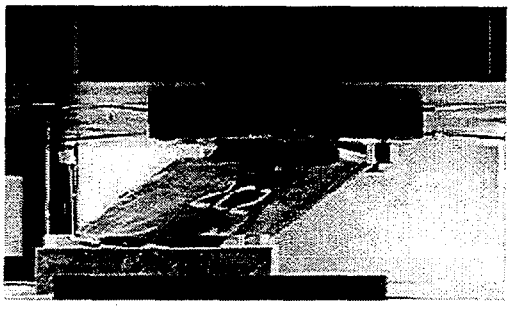

Figure 5-a. Compression and shear test at 200% shear strain on an optimized HDRB with recess attachment system

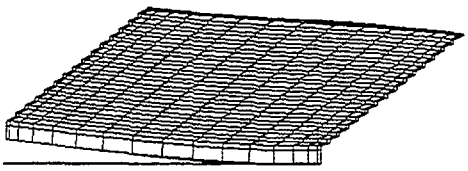

Figure 5-b. A quarter FEM of an optimized HDRB with recess attachment system at 200% shear strain

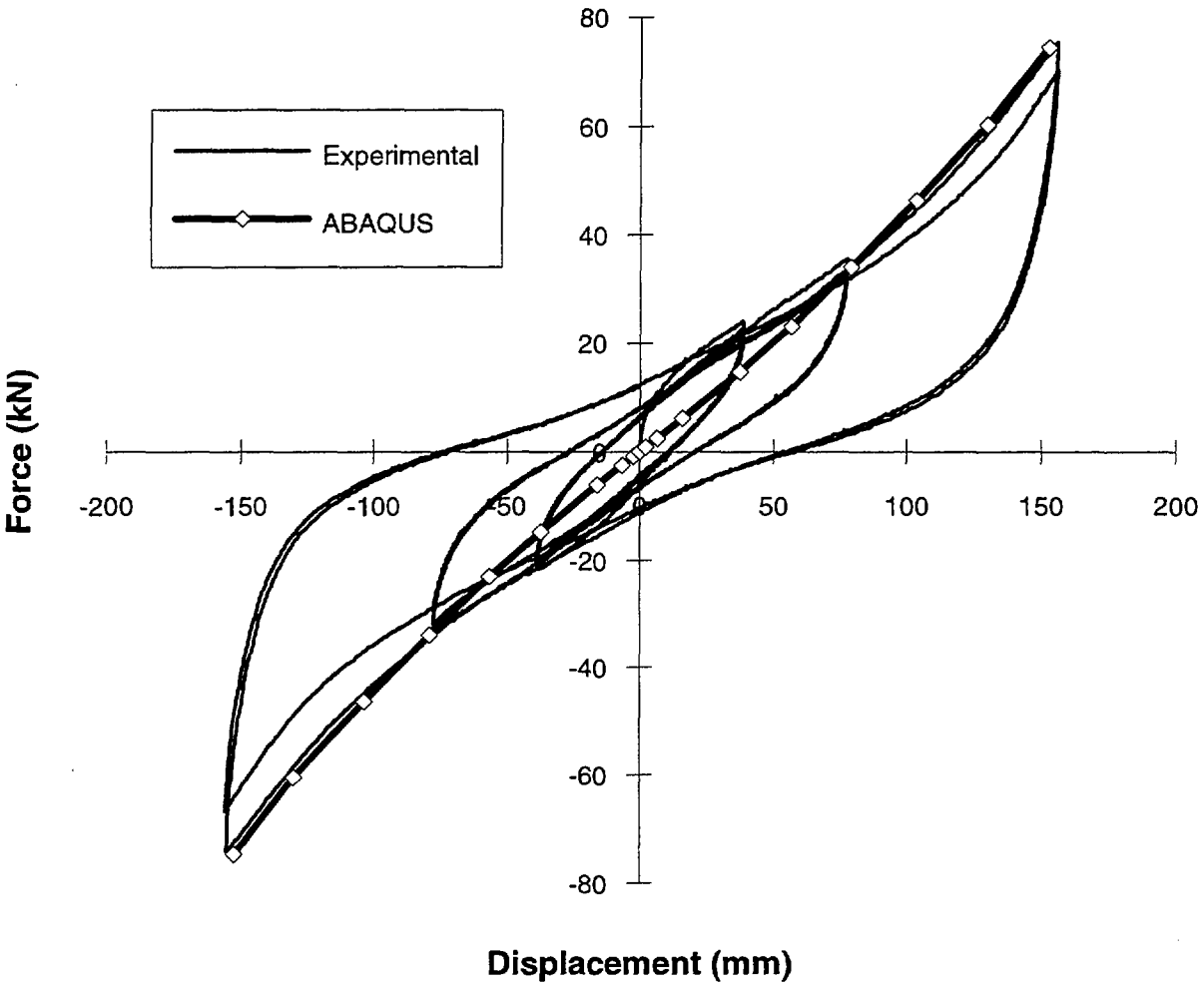

Figure 5-c. Experimental and numerical force-displacement values for a combined compression & 200% shear strain test on an optimized HDRB (1:2 scale, diameter=250 mm, H=75 mm, S=24, G=0.8 MPa, recess attachment system)

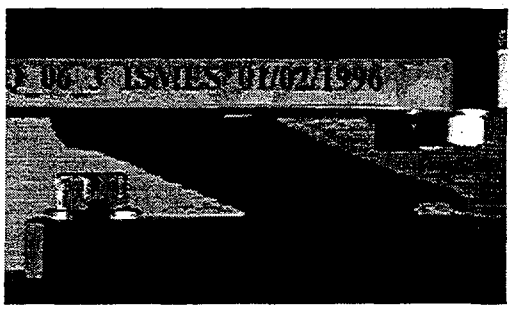

Figure 7-a. Compression and shear test at 400% shear strain on a bolted 'futher optimized' HDRB

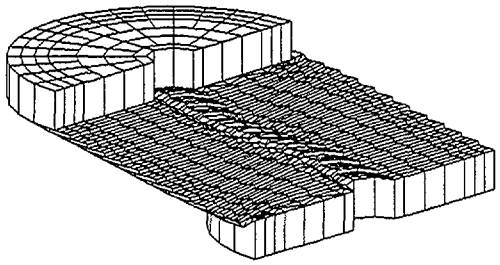

Figure 7-b. FEM of a bolted 'further optimized' HDRB at 400% shear strain

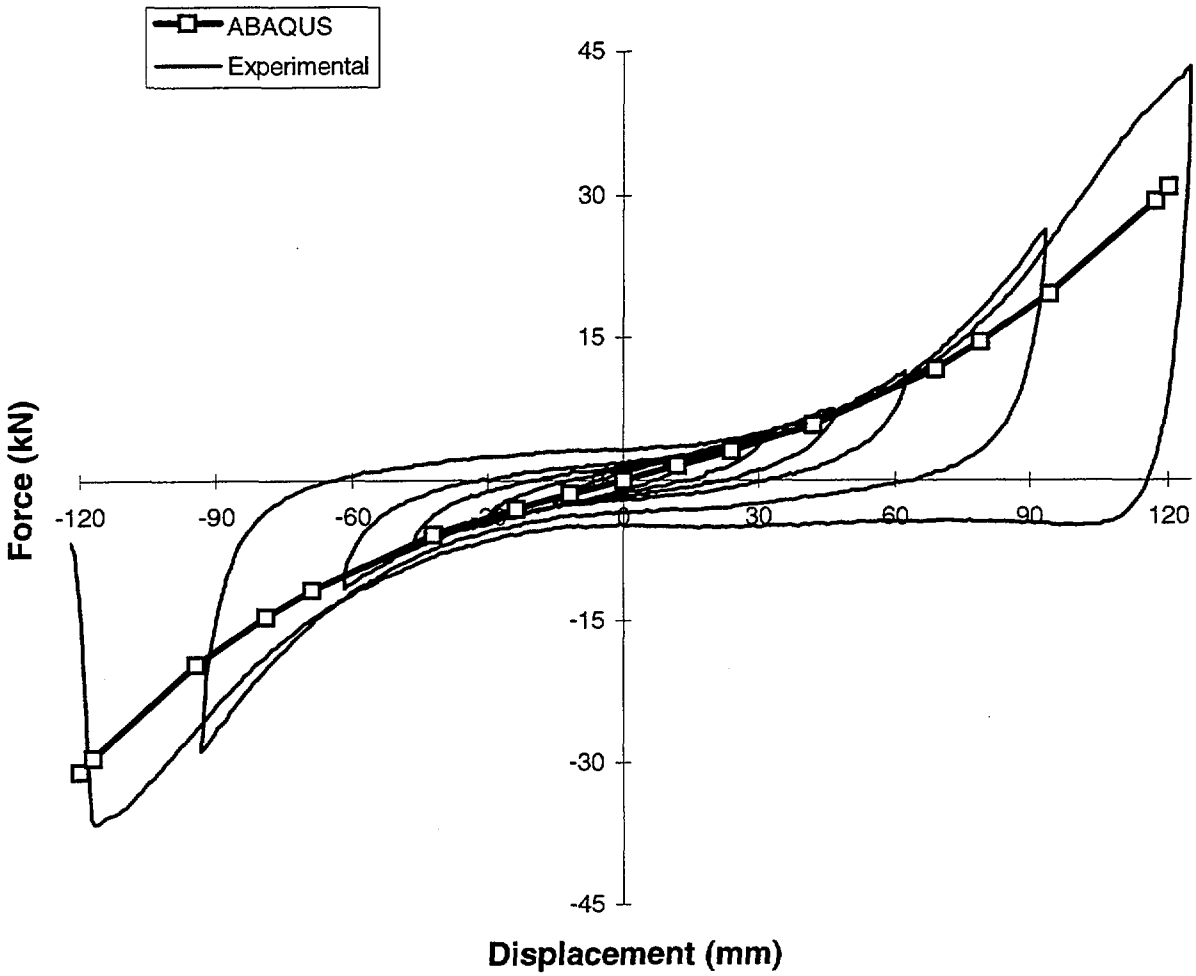

Figure 7-c. Experimental and numerical force-displacement values for a combined compression & 400% shear strain failure test on a bolted 'further optimized" HDRB (1:4 scale, diameter=125 mm, H=30 mm, S=12, G=0.4 MPa)